Journal Pre-proof

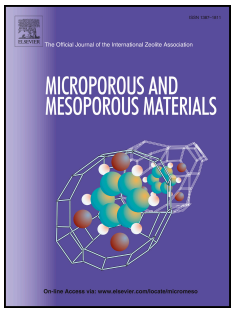

A green and reusable catalytic system based on silicopolyoxotungstovanadates incorporated in a polymeric material for the selective oxidation of sulfides to sulfones

Romina Alejandra Frenzel, Valeria Palermo, Angel Gabriel Sathicq, Asma M. Elsharif, Rafael Luque, Luis René Pizzio, Gustavo Pablo Romanelli

PII: S1387-1811(20)30584-9

DOI: https://doi.org/10.1016/j.micromeso.2020.110584

Reference: MICMAT 110584

To appear in: *Microporous and Mesoporous Materials*

Received Date: 24 April 2020

Revised Date: 6 August 2020

Accepted Date: 21 August 2020

Please cite this article as: R.A. Frenzel, V. Palermo, A.G. Sathicq, A.M. Elsharif, R. Luque, Luis.René. Pizzio, G.P. Romanelli, A green and reusable catalytic system based on silicopolyoxotungstovanadates incorporated in a polymeric material for the selective oxidation of sulfides to sulfones, *Microporous and Mesoporous Materials* (2020), doi: https://doi.org/10.1016/j.micromeso.2020.110584.

Romina Alejandra Frenzel and Valeria Palermo performed all experiments in the lab and prepared the first draft

Angel Gabriel Sathicq performed several materials characterisations and prepared the first draft

Rafael Luque designed the methodology, contributed to the first draft and revised and completed the final draft for submission

Luis René Pizzio supervised all students, experiments, provided funding for the experiments and contributed to the first and final draft

Gustavo Pablo Romanelli was in charge of students supervision, provided lab resources, validated results and revised the final draft

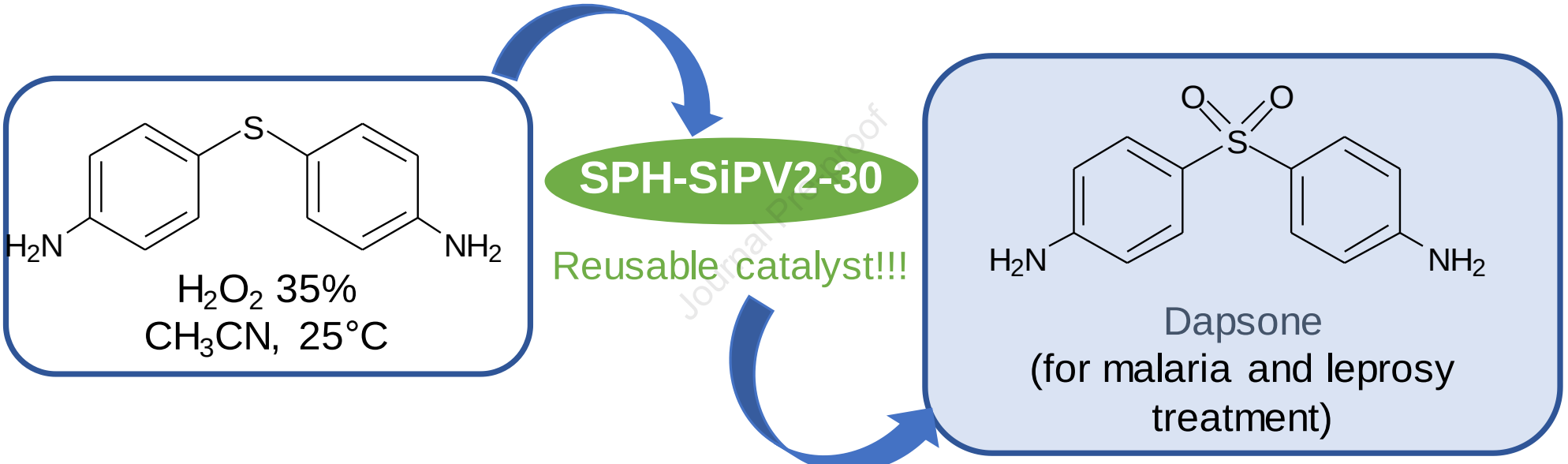

A green and reusable catalytic system based on silicopolyoxotungstovanadates incorporated in a polymeric material for the selective oxidation of sulfides to sulfones

Romina Alejandra Frenzel[a], Valeria Palermo[a], Angel Gabriel Sathicq[a], Asma M. Elsharif[b], Rafael Luque[c,d], Luis René Pizzio[a,**], Gustavo Pablo Romanelli[a,e,*]

[a]*Centro de Investigación y Desarrollo en Ciencias Aplicadas "Dr. Jorge J. Ronco" CINDECA, (CONICET-CIC-UNLP), Facultad de Ciencias Exactas, Universidad Nacional de La Plata, Calle 47 N° 257, B1900AJK, La Plata, Argentina.*

[b]*Department of Chemistry, College of Science, Imam Abdulrahman Bin Faisal University, P.O. Box 1982, Dammam, 31441, Saudi Arabia*

[c]*Departamento de Química Orgánica, Grupo FQM-383, Universidad de Córdoba, Campus de Rabanales, Edificio Marie Curie (C-3), Ctra Nnal IV-A, Km 396, 14014 Córdoba, Spain*

[d]*Scientific Center for Molecular Design and Synthesis of Innovative Compounds for the Medical Industry, Peoples Friendship University of Russia (RUDN University), 117198 Moscow, Russia*

[e]*Cátedra de Química Orgánica, Facultad de Ciencias Agrarias y Forestales, Universidad Nacional de La Plata, Calles 60 y 119 s/n, B1904AAN La Plata, Argentina.*

* Corresponding author.

** Corresponding author.

E-mail addresses: gpr@quimica.unlp.edu.ar (G.P. Romanelli), lrpizzio@quimica.unlp.edu.ar (L.R. Pizzio)

Abstract

Two vanadium-containing Keggin silicopolyoxotungsto compounds $K_5SiVW_{11}O_{40}$ and $K_6SiV_2W_{10}O_{40}$ were synthesized and characterized. They were incorporated in a superporous hydrogel constitute by prop-2-enamide and propenoic acid as initial monomers and bis-acrylamide as cross-linking moiety. Materials were characterized by several techniques. According to FTIR and ^{51}V MAS-NMR, the $(SiV_xW_{12-x}O_{40})^{(4+x)-}$ anions are the main species present in the hybrid materials. Additionally, they do not decompose during the preparation of the composite. XRD and SEM-EDX results suggest that $(SiV_xW_{12-x}O_{40})^{(4+x)-}$ anions were well dispersed in the support or present as amorphous phases. These materials were evaluated as catalysts in the oxidation of sulfides to sulfones, using an eco-friendly oxidant and mild reaction conditions. The hybrid materials with higher content of the heteropoly compound displayed a remarkable catalytic behaviour in the oxidation of diphenyl sulfide. Materials also exhibited a stable catalytic performance through consecutive reuses. Optimum reaction parameters established were subsequently translated to the oxidation of a sulfide of interest (dapsone) due to its pharmacological activities.

Keywords

Keggin silicopolyoxotungsto compounds, superabsorbent hydrogel, sulfide oxidation, dapsone.

1. Introduction

The oxidation of sulfides is an extensively studied procedure due to the relevance of obtained products (sulfoxides and sulfones) as reaction intermediates in synthetic organic chemistry. Both products are widely used in the formation of biologically active molecules such as pharmaceuticals and pesticides [1-3]. For example, derivatives of phenyl tribromomethyl sulfone have been described as plant fungicide and diiodomethyl *p*-tolyl sulfone as an algaecide, bactericide, and fungicide [4,5]. In the pharmaceutical field, sulfones are important in the treatment of several diseases, such as diabetes [6], leprosy and malaria [7,8], in dermatology [9], and as reaction intermediates in the production of more complex molecules such as sulphonamides, used as antibiotics in clinical practice [10,11]. This highlighted the importance of such compounds and the need to find simple and eco-friendly processes to synthesize them.

Sulfones are usually prepared by the oxidation of a precursor sulfide [12], using an oxidizing system. The oxidizing agent generally used includes potassium permanganate, peracids, $NaIO_4$, CrO_3, MnO_2, among others [13-15]. However, the use of an oxidative route excludes the presence of oxidation-sensitive functional groups, and generally involves long reaction times, the use of harmful or expensive oxidants, undesirable side reactions at other functional groups and low yields. To avoid the generation of large amounts of dangerous waste resulting from the classical procedure, stoichiometric oxidants can be replaced by eco-friendly environmental catalytic systems, using a green oxidant such as hydrogen peroxide, organic peroxide and molecular oxygen, which provide many benefits compared to other oxidants [16,17].

The main advantage of using H_2O_2 as oxidant is the production of water as the only by-product. Since in general the no catalyst reactions are slow, numerous catalytic systems have been reported for the hydrogen peroxide oxidation of sulfides, including various metal complexes of transition metals and lanthanides [18-20]. POMs (polyoxometalates) were reported as outstanding acid and oxidation catalysts since their remarkable acidic and redox properties [17,21]. Particularly, W-based polyoxometalates showed to be effective catalysts for the oxidation of phenols, alcohols, and olefins using hydrogen peroxide as oxidant [21,22]. The main disadvantage of POMs as catalysts is their hard recovering and reusing due to their high solubility in polar solvents. This issue was overcome by their immobilization in appropriate porous materials with suitable textural properties such as mean pore diameter specific surface area [23,24].

In the present work, a superporous hydrogel was used as support. The existence of this type of polymer is well known but only a few of them have been reported to be used in the catalysis field [25-28]. They are commonly employed as drug delivery systems in medicine or biotechnology [29-31]. There is a variety of different superporous hydrogels, depending on the precursor monomers, the nature and concentration of the cross-linking agent, and the initiator type.

The incorporation of a vanadium atom in the structure of POM improves the catalytic activity of the material owing to the oxidative properties of vanadium and because it increases the acidity of the material.

We previously reported the synthesis of phosphomolybdic acid doped with vanadium to be used as catalyst in the synthesis of 4-dihydropyrimidin-2-(1H)-thiones/-ones [32]. The enhancement in the catalytic performance of these materials in comparison with the acid without vanadium encouraged us to prepare Keggin-type silicopolyoxotungsto compounds modified by replacing tungsten atoms by vanadium and included them in a superporous hydrogel as support.

The catalytic activity of synthesized materials in the oxidation of diphenyl sulfide (DPS), using hydrogen peroxide as oxidant (Scheme 1). The reaction parameters were investigated to obtain the optimum reaction conditions in the selective oxidation of DPS. These conditions were subsequently translated to the oxidation of 4,4'-diaminodiphenyl sulfide to synthesize a well-known drug used for malaria and leprosy medical treatment (dapsone, Scheme 2).

2. Experimental

2.1. Synthesis of SPOV (vanadium silicopolyoxotungsto compounds)

2.1.1. Synthesis of SiPV1 ($K_5(SiVW_{11}O_{40})$)

The synthesis of SiPV1 was performed according to literature data [33]. For this purpose, a solution of 20.8 g (7.2 mmol) of SiP ($H_4SiW_{12}O_{40}$) in 12 mL of distilled water at 80°C was prepared. Afterwards, 6.8 g $NaHCO_3$ was added slowly until a pH value of 8.5 was attained. A second solution, prepared by mixing 2.4 g (200 mmol) of $NaVO_4$ and 6 mL of HCl 6 M, was added slowly to the first solution. Then, 1.6 g of KCl was added. After filtration, the orange solid was washed with distilled water and dried at 25°C under reduced pressure, until constant weight.

2.1.2. Synthesis of SiPV2 ($K_6(SiV_2W_{10}O_{40})$)

The synthesis of SiPV2 was conducted following the procedure reported [34]. Firstly, the lacunary phase SiPW9 ($Na_{10}(SiW_9O_{34})$) was prepared following a previous protocol [35]. A water solution (50 mL) of Na_2WO_4 (45.4 g, 154 mmol) and Na_2SiO_3 (2.7 g, 22 mmol) were prepared. Subsequently, the pH value was taken to 4.5 using HCl 6 M, heated 1 h at 80°C and filtered. A water solution (12 mL) of Na_2CO_3 (12.0 g) was slowly poured. After magnetic stirring at 60°C,-the white solid formed was filtered, washed with 10 mL of cold ethanol and dried at 25ºC under vacuum at until constant weight. 4.0 g of the obtained solid (SiPW9) and 0.5 g of $NaVO_3$ were subsequently dissolved in 40 mL of distilled water. The pH was adjusted to 1.5 using HCl 6 M, and 5.0 g of KCl was added under vigorous stirring. Finally, 150 mL of cold ethanol was added, forming an orange solid. This solid was filtered, washed with 10 mL of cold ethanol and dried at 25°C under reduced pressure until constant weight.

2.2. Synthesis of the SPH-SPOV hybrid materials

The superporous hydrogel (SPH) was synthesized according to the technique reported in previous work [36]. For SPH classic synthesis, the following aqueous solutions were mixed into a reaction-tube at 25°C, with vigorously stirring: 300 µL of prop-2-enamide 50%, 200 µL of propenoic acid 50%, 70 µL of N,N-methylene bis acrylamide (bis-acrylamide) 2.5%, 300 µL of SPOV solution (10%, 20%, or 30% w/w), 25µl of ammonium persulphate 20%, 25 µL of N,N,N',N'-tetramethylethylendiamine 20% and 100 mg of $NaCO_3H$.

The polymerization was completed 10 minutes after the addition of all components. Finally, the solids were dried at 100ºC, until constant weight. The samples are labelled SPH-SiPV1-X and SPH-SiPV2-X, where X is the content of SPOV incorporated (X = 10%, 20%, or 30% w/w). The procedure to obtain the SPOV amount into the hybrid material is described in complementary material.

2.3. Characterization

2.3.1. FTIR analysis

Samples were ground, mixed with BrK (1% of sample), and formed pellets. FTIR spectra of the were collected in transmission mode in the range of 400-4000 cm^{-1} employing a Bruker IFS 66.

2.3.2. Raman spectroscopy

Raman spectra of the samples were recorded in the 100–1100 cm^{-1} range using a Raman microprobe equipped with a photodiode array detector at 25°C.

2.3.3. X-ray diffraction analysis (XRD)

X-ray powder diffraction of the samples were performed employing a Philips PW-1732, using Cu Kα radiation, in the range 5°- 60° of 2θ.

2.3.4. Nuclear magnetic resonance (^{51}V MAS-NMR)

The ^{51}V magic angle spinning nuclear magnetic resonance of the solids was recorded in Bruker Avance II-300 equipment. The working frequency used was 78.89 MHz, 3.5 μs

pulses and a repetition time of 5 s. The spin rate was 8 and 10 kHz, and 1024 pulse responses were collected for each experiment, using V_2O_5 as external reference.

2.3.5. Diffuse reflectance spectroscopy (DRS)

Diffuse reflectance spectroscopy spectra of the samples were collected using a Lambda 35, Perkin Elmer spectrophotometer (see supplementary information for more details). The Eg (absorption edge energy) was estimated from the DRS-UV-vis employing the Kubelka-Munk remission function (F(R ∞)) and $(F(R\ \infty)h\upsilon)^{1/2}$ [37, 38].

2.3.6. Acidity measurements

Potentiometric titration was used for measuring the acid strength and the number of acid sites of the solid samples. More details about the technique and the ranges used for the classification of the sites according to the acid strength [39] were added in the supplementary information file.

2.3.7. Nitrogen adsorption-desorption isotherms

N_2 isotherms (adsorption-desorption) of the samples were collected using a Micromeritics Asap 2020 equipment. These results were used to estimate the specific surface area (S_{BET}), using the Brunauer–Emmett–Teller model and the mean pore diameter (Dp) using the BJH method. The pore size distribution (PSD) was calculated using the density functional theory (DFT) method.

2.3.8. Scanning electron microscopy with energy dispersive X-ray spectroscopy (SEM-EDX).

Secondary electron micrographs of the samples were obtained by scanning electron microscopy (SEM) using a Philips 505 instrument. Energy dispersive X-ray analysis (EDX) of the samples was obtained using an EDAX 9100 analyzer at a working potential of 15 kV.

2.4. Catalytic test

2.4.1. General remarks

The used chemicals were all reagent grade pure, purchased from Merck and Aldrich. The products and the unreacted organic substrates were quantified by gas chromatography (GC), and the reaction progress was monitored by thin layer chromatography analysis. The diphenyl sulfone was identified by GC-MS using Perkin-Elmer equipment, and dapsone was identified by ^{1}H NMR and ^{13}C NMR using a Varian Mercury Plus 200 spectrometer. As a complement to the above spectral data, we performed melting point determinations (the product identification can be found in the supplementary information). Hydrogen peroxide (H_2O_2 35% w/v, aqueous solution) was used as oxidant. The concentration of the peroxide solution was estimated by iodometric titration.

2.4.2. General procedure for the catalytic oxidation of sulfides to sulfones

1 mmol of organic substrate (185 mg of DPS), 5 mL of the solvent (acetonitrile), SPOV/SPH-SPOV as catalysts and variable amounts of H_2O_2 35% w/v at 25°C were added in a test tube. The substrate:SPOV molar ratio used was 100:1, both in homogeneous (SiPV1 and SiPV2) and heterogeneous (SPH-SiPV1 and SPH-SiPV2) media. The studied variables to obtain the optimum conditions were amount of catalyst, substrate/oxidant ratio

and reaction time (the complete experimental conditions are detailed in the supplementary information).

2.4.3. Catalyst reuse

The reusability of the catalysts was evaluated in three consecutive runs, using the optimum reaction conditions. The catalyst was isolated from the reaction mixture, after each run, washed twice with the solvent (2 mL), dried under vacuum at 25°C until constant weight, and then reused in a new experiment.

3. Result and discussion

3.1. Materials characterization

Figure 1 presents the infrared spectra of SiP, SiPV1, and SiPV2 in absorbance mode (transmittance data were converted to absorbance and each spectrum normalized to the band associated to Si-O_a stretching). The infrared bands of $(SiW_{12}O_{40})^{4-}$ can be assigned to the Keggin structure, in agreement with literature reports: 1019, 980, 926, 883, 781, and 540cm^{-1}, the first one is not assigned, and the next corresponding to W-O_d, Si-O_a, W-O_b-W and W-O_c-W stretching vibrations as well as W-O-W bending vibration, respectively [40,41]. The different oxygens include: a) bridging W and Si, b) corner sharing, c) edge sharing, and d) terminal.

For SiPV1 and SiPV2, the infrared spectra exhibited the characteristic bands between 700 and 1010 cm^{-1} due to metal-oxygen absorption stretching vibrations. The presence of these bands indicates that the primary structure was retained upon vanadium incorporation. For

SiPV1, bands corresponded to 1005 cm^{-1}, 962 cm^{-1} (W-O_d), 916 cm^{-1} (Si-O_a), 892 cm^{-1} (sh, W-O_b-W), 779 cm^{-1} (W-O_c-W), 518 cm^{-1}, and 474 cm^{-1}, while for SiPV2 1007 cm^{-1}, 970 cm^{-1} (W-O_d), 918 cm^{-1} (Si-O_a), 892 cm^{-1} (sh, W-O_b-W), 787cm^{-1} (W-O_c-W), 611 cm^{-1}, 530 cm^{-1}, and 473 cm^{-1}. Si–O_a and W–O_d bands presented a slight shift to lower frequencies with respect to SiP values, and the intensities of W-O_b-W and W-O_d bands decreased with the incorporation of V, which could be attributed to the increase of the negative charge of the anion (weakening these bonds). The intensity of W-O_c-W bands increased; and the incorporation of two vanadium atoms produced a positive shift in this stretching band, a split in W-O-W bending vibration. These modifications are due to vanadium incorporation into the primary Keggin structure, in good agreement with literature data [34,42].

Figures 2 and 3 show the FTIR spectra of SiPV1, SiPV2 and the hybrid materials SPH-SiPV1-X and SPH-SiPV2-X, respectively. Therefore, the appearance of the characteristic bands of the Keggin structure overlapping those belonging to SPH indicates the success achieved in the synthesis of SPH-SiPV1-X and SPH-SiPV2-X materials. For the hybrid materials, the bands corresponding to SiPV1 and SiPV2 are present in SPH-SiPV1-X and SPH-SiPV2-X, respectively, with a lower intensity due to the dispersion of SPOV in the polymer matrix. Moreover, the intensity of the FTIR bands rises with the content of SiPV1 (or SiPV2) in the SPH.

Figure 4 presents the Raman spectra of the bulk SPOV. The bands at 991 cm^{-1} and 980 cm^{-1} are assigned to symmetric and asymmetric stretching (ν W-O_d). Also, two weak bands are observed at 899 cm^{-1} (ν_{as} W-O_b-W) and 544 cm^{-1} (ν_{as} W-O_c-W) [43]. The stretching

vibration of the W-O_d bond presents a shift with respect to $K_4(SiW_{12}O_{40})$ due to vanadium incorporation [44].

The XRD diagrams obtained for SPH-SPOV samples do not display the characteristic diffraction lines of SiPV1 and SiPV2, being similar to the XRD pattern of the SPH. From these results, it can be inferred that SPOV is highly dispersed into the sample or as a noncrystalline phases (data not shown) [45, 46]. This is in agreement with EDX mapping images of W element in the SPH-SPOV samples (Figure S1) that shows its overall homogeneous distribution.

Figure 5 shows the ^{51}V MAS-NMR spectra obtained for SiPV1 and SiPV2. In both cases, they are composed of two predominant lines at δ = -542 ppm and -503 ppm for SiPV1, and δ = -546 ppm and -503 ppm for SiPV2. The presence of two bands is assigned to the existence of vanadium replacing two different kind tungsten atoms in the Keggin anion. The obtained bands agree with the ones reported in the bibliography [43,47], with a shift to lower δ values, due to the arrangement of potassium atoms in the synthesized compounds.

Table 1 show the S_{BET} (specific surface areas) and mean pore diameter (Dp) of SPOV, SPH and the synthesized materials, estimated from N_2 isotherms using the BET method. The values obtained for the bulk materials range from 5 m^2/g to 17 m^2/g, being common values for POMs, in agreement with the literature values [48].

S_{BET} values of the hybrid materials are similar to that of SPH (341 m^2/g) value, decreasing slightly with the increase of SPOV content. Dp values remains practically constant. The continuous decrease in S_{BET} could be due to the clogging of hydrogel pores by the polyoxoanions. The increase in the S_{BET} values for the SPH-SPOV-X hybrid materials represents an advantage in the use of them in heterogeneous catalysis. The isotherms of

SPH-SiPV2-X and SPH-SiPV1-X materials (Figure S2) can be classified as type IV (with H1 hysteresis loops), characteristic of mesoporous materials. The increase of N_2 adsorbed in the 0.8-1 range of P/Po is associated with the presence of large mesopores. The pore size distribution obtained by the DFT method shows that the pores are mainly between 2 and 4 nm in size (centered at ~3.6 nm). Large mesopores (between 12 and 20 nm) are also present (Table 1), although their pore volume is rather small. Neither the main features of the isotherms nor PSD seems to be affected by the SPOV content.

SEM micrographs of SPH and SPH-SiPV1-30 hybrid materials (Figure 6) show a sponge-like morphology conformed by a network of cross-linked channels. From their comparison, the incorporation of SPOV during the synthesis of SPH-SPOV-X materials did not significantly influence such sponge-like structure.

The absorption spectra of non-reduced heteropolyanions obtained by DRS-UV-vis in the 200-600 nm region consists of bands that may be assigned to oxygen-to-metal transfers.

DRS spectrum of bulk SiP presents two broad bands, the first one is below 250 nm and the other extends from 250 nm to 400 nm, which are assigned to the charge transfer from bridging or terminal O 2p to W 5d (W-O-W and W-O_d) respectively [42,43,49]. When V atom is included in the primary Keggin unit, the observed absorption extends to the visible spectrum. SiPV1 and SiPV2 DRS spectra show the absorption threshold onset continuously shifted to the visible region (Figure 7). The displacement increases with the increment of the number of V atoms per Keggin anion.

For the synthesized hybrid materials, the absorption bands of SPOV are overlapping with the SPH spectrum. Moreover, the absorption band extension depends on the SPOV content in the composite (Figures 7 (A) and (B)).

The absorption edge energy (Eg), calculated from DRS-UV-vis spectra by means of the remission function of Kubelka-Munk, is a useful parameter to estimate the reduction potentials of POMs [37,49]. Vanadium incorporation in the POM framework stabilized the lowest unoccupied molecular orbital (LUMO) since vanadium *d*-orbitals are assumed to be more stable than tungsten ones, enhancing the catalytic activity in the oxidation reaction [50], which is reflected in the lower Eg values obtained for the SPOV. Table 2 shows the Eg values for the SPOV and SPH-SPOV materials. Owing to the increment of SPOV content in the samples, there is a decrease in the absorption edge energy, which is translated into a stronger oxidizing capacity (more easily reduced).

The potentiometric titration results (Figure 8) of the prepared materials present the following relative order of the maximum acid strength (MAS): SiPV1>SPH-SiPV1-30>SPH-SiPV1-20>SPH-SiPV1-10. The same order was observed for the SPH-SiPV2 series, with an increase in the Ei values due to the increment in the number of V atoms in the $(SiV_XW_{12-X}O_{40})^{(4+X)-}$ anion. According to the initial potential of the electrode (80 mV and 110 mV) the acid sites present in SiPV1 and SiPV2 can be classified as strong and very strong respectively. The acid sites present in the rest of the synthesized materials are classified as strong acid sites, in agreement with the literature data [39].

Additionally, the MAS of the SPH-SiPV1-10 (Ei = 15 mV), SPH-SiPV1-20 (Ei = 31 mV), and SPH-SiPV1-30 (Ei = 52 mV) composites are higher than SPH (Ei = −4 mV), but lower

than that of SiPV1 (Ei = 80 mV). A similar behaviour is observed for SPH-SiPV2 materials.

For both series of hybrid materials, the Ei value increased in parallel with the amount of SPOV included in the composite (Figure 8).

3.2. Catalytic activity tests

As first test of the catalytic activity, a blank experiment was carried out using an excess of oxidant. After 24 h of reaction only 5% of DPS conversion was detected (Table 3, entry 1). The effect of the support on sulfide conversion was evaluated using SPH as catalyst. In this case, the conversion value was similar to that of the blank experiment (Table 3, entry 2).

Furthermore, the catalytic activity of the bulk materials (SiPV1 and SiPV2) was tested using 1 mmol of substrate (DPS), acetonitrile (5 mL), excess of H_2O_2 35% w/v (1 mL) and 25°C. The synthesized SPOV showed an excellent catalytic performance with 66% and 96% of sulfide conversion, after 7 h, for SiPV1 and SiPV2 respectively (Table 3, entries 4 and 5). As we showed previously, the oxidation capacity, estimated from DRS-UV–vis, increases with the number of V in the PMO. These results evidence the enhancement of the catalytic activity when more than one vanadium atom was introduced in the $(SiV_XW_{12-X}O_{40})^{(4+X)-}$ anion.

Table 4 shows additional tests carried out to evaluate the reaction time under the same conditions used previously: SiPV1 and SiPV2 as catalysts, excess of H_2O_2 35% w/v, 25°C and four different reaction times: 5 h, 7 h, 9 h, and 24 h, respectively. With both catalysts, the selectivity is towards the sulfoxide at short reaction times, and as it increases, the

selectivity favors the sulfone formation. Moreover, SiPV2 catalyst turned out to be more active than SiPV1, reaching 100% of sulfide conversion at 9 h with 100% selectivity to sulfone (Table 4, entries 2), while the same conversion results using SiPV1, the reaction time increases to 24 h (Table 4, entries 1). The enhancement in the catalytic activity of the vanadium-containing POMs is related to their acidity. In previous work, we found that an increase in the acidity of the POMs and heteropoly acids is translated into a better catalytic performance, since the formation of the peroxo-metal intermediate between the peroxide and the catalyst is favored in the presence of the vanadium atom [32,51,52].

During the optimization of the oxidation reaction, the substrate/catalyst amount ratio used was evaluated. The tested catalyst amounts were 0.5%, 0.7%, 1%, and 1.5%, employing the same aforementioned conditions. As seen in Figure 9, the conversion of the substrate increased with the increment of the catalyst amount, reaching a plateau when 1% of SiPV2 was used. Table 5 shows that using lower amounts of SiPV2 as catalyst, the selectivity toward diphenyl sulfoxide were 72% and 68% when 0.5% and 0.7% catalyst amounts were used, respectively (Table 5, entries 1 and 2). While, with 1% of SiPV2, 100% selectivity toward sulfone was achieved (Table 5, entry 3). On the other hand, no relevant changes were observed using 1.5% of catalyst amount (Table 5, entry 4).

The influence of the substrate/H_2O_2 ratio in the oxidation reaction of DPS is presented in Table 6. The conditions tested were: 1 mmol of DPS, acetonitrile as solvent, 1% mmol of SiPV2, 25°C and variable DPS/H_2O_2 ratios (1:3, 1:5, 1:7, and 1:10 respectively). Excellent conversion values could be obtained for all substrate/peroxide ratios studied. Although all tests gave conversions greater than 70% (Table 6, ent. 1-4), a mix of products (sulfoxide

and sulfone) was obtained when quantities lower than 1 mL (1:10 ratio) was used. A total conversion of sulfide was reached with 100% sulfone selectivity when a 1:10 substrate/peroxide ratio was tested, (Table 6, entry 4).

Although optimum reaction conditions could be found, the greatest disadvantage of the use of these materials is that the SPOVs are completely soluble acetonitrile, so the recovery of the catalyst is rather complex and requires the use of extra solvent and reaction steps.

In view of environmental and economic concerns, we tested the hybrid materials synthesized in the present work as heterogeneous catalysts in the oxidation of DPS using optimum conditions found previously for bulk materials.

The conversion and selectivity achieved using SPH-SiPV1-X and SPH-SiPV2-X hybrid materials were lower, and the reaction times longer as compared to those of SPOV in homogeneous conditions (Table 7). Moreover, the conversion value increased in correspondence with the rise of the SPOV content and the catalysts are able to be simply recovered from the reaction mixture. Only the materials with higher SPOV content (SPH-SiPV1-30 and SPH-SiPV2-30), showed great conversion values, with 79% and 94% of DPS conversion and 90% and 100% selectivity to sulfone, respectively (Table 7, entries 4 and 7). The order in the oxidation capacity in the catalytic test, related to SPOV content, is that expected according to the Eg values obtained in the characterization of the samples, and agrees with the order obtained in the acidity measurements:

SPH-SiPV1-10<SPH-SiPV1-20<SPH-SiPV1-30 (the same behaviour was depicted for the SPH-SiPV2-X samples). The incorporation of vanadium in the primary structure of Keggin heteropolyacids and POMs was reported to increase N_{AS} (the number of acid sites). In this way, a correlation between the N_{AS} and the conversion values was observed [50,51].

The reusability is the most valuable characteristic of a solid heterogeneous catalyst. In general, the catalytic activity decreases with the repeated use and depends on many factors, such as active compound leaching and catalytic neutralization.

To evaluate the reusability of SPH-SPOV-X, the SPH-SPOV-X catalyst was recovered and reused under identical reaction conditions. For this purpose, SPH-SPOV-X was filtered from the reaction mixture upon reaction completion, washed with the solvent and dried under reduced pressure at 25°C until constant weight. The results obtained for the first, second and third reuses are summarized in Table 8.

SPH-SiPV2-30 was refluxed in acetonitrile (5 mL) for 24 h, filtered and dried under reduce pressure till constant weight to further evaluate potential SiPV2 solubilisation from the catalyst. No appreciable changes in conversion and selectivity values were detected when the treated catalyst was used. DPS conversion was 92% and 94% for the treated and fresh catalysts respectively with 100% selectivity for both materials (Table 9, entries 1 and 2). Acetonitrile was used as solvent to evaluate DPS oxidation under reflux conditions without the addition of SPH-SiPV2-30. After 24 h, only 10% of DPS conversion was detected (Table 9, entry 3), an analogous value to that of the blank experiment (Table 3, entry 1).

To conclude, an additional test was made to verify the catalyst leaching. The reaction was stopped at 3 h (before it was complete), the catalyst was filtered off and the reaction continued for 7 h. The measured DPS conversion was comparable to that at 3 h (68% and 69%, respectively). These experiments proved that SiPV2 was not leached from SPH-SiPV2-30 catalyst, with the proposed system being highly stable and reusable under the investigated reaction conditions.

Upon optimisation of the reaction conditions for the selective oxidation of DPS, subsequent selective oxidations were conducted to obtain dapsone (Scheme 3), using 1 mmol of 4,4'-diaminodiphenyl sulfide, 5 mL of acetonitrile, 1 mL of H_2O_2 35% w/v, 1% mmol of SPH-SiPV2-30 as heterogeneous catalyst, 25°C and 24 h. When the reaction was completed, the catalyst was removed, the solvent was evaporated and the product was easily isolated from the reaction mixture. Purification was made by recrystallization from ethanol, allowing a 72% yield of pure dapsone. The product was characterized by ^{1}H NMR and ^{13}C NMR spectroscopy. Experimental and characterization are specified in the supplementary information.

Table 10 lists some of the methods reported in the literature for dapsone synthesis. In general, all include several reaction steps, due to the necessity of protecting the amino group. The whole sequence is often protection-oxidation-deprotection, using a strong and

corrosive acid such as H_2SO_4 (c), strong oxidizing agents or high temperatures (Table 10, entry 2). The conditions used for the typical syntheses involve the use of extra solvent, reagents and the generation of unnecessary waste (Table 10, ent. 3 and 4) [53-55].

In the present work, the synthesis of 4,4'-diaminodiphenyl sulfone was carried out using low temperatures, cheap and easily available reagents, with catalytic systems being able to be used a minimum three times without any activity loss. The oxidation reaction occurs in only one step, due to the selectivity of the catalyst to the sulfide, and the yield obtained is comparable or improved to those previously reported (Table 10, entry 1).

4. Conclusions

Two series of Keggin-based hybrid materials were synthesized by the inclusion of SiPV1 and SiPV2 into a superporous hydrogel. FTIR results revealed that SiPV1 and SiPV2 were successfully incorporated into the superporous hydrogel. The surface area of the hybrid materials SPH-SPOV showed a remarkable increase in comparison with the bulk SPOV compounds, which represents a great advantage in the heterogeneous catalysis field.

The synthesized materials were evaluated as catalysts in the DPS oxidation to diphenyl sulfone, using aqueous H_2O_2 35% w/v as green oxidant. They showed a great catalytic performance under mild reaction conditions, being able to selectively obtain the sulfone. In order to simplify the recovering of the catalyst after the reaction ended, the hybrid materials were employed as heterogeneous catalysts, representing a significant advantage in operational simplicity, the cleanness of the reaction and very good yield toward dapsone synthesis.

A correlation cold also be established between catalytic oxidation activity and absorption edge energy (Eg) of the catalysts, demonstrating Eg could be used as correlation parameters for the reduction potentials of the materials, evidence of catalytic oxidation potential for POM-based catalysts.

Supplementary information

The procedure of the hydrogel synthesis is descripted. Also, the details of the potentiometric titration technique are explained. The experimental conditions used in the selective oxidation of sulfides are given, together with the characterization by ^{1}H NMR and ^{13}C NMR spectroscopy. Finally, W elemental mapping images and N_2 adsorption-desorption isotherms are shown.

Declaration of competing interest

The authors declare that they have no conflict of interest.

CRediT authorship contribution statement

R.A. Frenzel: Methodology, investigation, data curation, formal analysis, writing - original draft. V. Palermo: Investigation, formal analysis, writing - review & editing. A.G. Sathicq:

Methodology, supervision, data curation, formal analysis. A.M. Elsharif: data curation, formal analysis, writing - review & editing. R. Luque: Conceptualization, writing - review & editing. L.R Pizzio: Conceptualization, methodology, supervision, formal analysis, writing - review & editing, funding acquisition, project administration. G.P. Romanelli: Conceptualization, methodology, supervision, formal analysis, writing - review & editing, project administration.

Funding

This work was supported by UNLP (X773), CONICET (PIP0449), and ANPCyT. The publication was prepared with support from RUDN University program 5-100.

Acknowledgments

The authors thank Lilian Osiglio, Graciela Valle, Mariela Theiller, and Edgardo Soto for the experimental measurements.

References

[1] H. Pellissier, *Tetrahedron* 62 (2006) 5559-5601. https://doi.org/10.1016/j.tet.2006.03.093

[2] A.J. Walker, *Tetrahedron: Asymmetry* 3 (1992) 961-998. https://doi.org/10.1016/S0957-4166(00)86026-7

[3] P. Devendar, G. Yang, *Top. Curr. Chem. (Z)* (2017) 375:82. https://doi.org/10.1007/s41061-017-0169-9

[4] K.M. Borys, M.D. Korzynski, Z. Ochal, *Beilstein J. Org. Chem.* 8 (2012) 259-265. https://doi.org/10.3762/bjoc.8.27

[5] M. Ema, T. Itami, H. Kawasaki, *Toxicol. Lett.* 62 (1992) 45-52. https://doi.org/10.1016/0378-4274(92)90077-W

[6] X. Chen, S. Hussain, S. Parveen, S. Zhang, Y. Yang, C. Zhu, *Curr. Med. Chem.* 19 (2012) 3578-3604. https://doi.org/10.2174/092986712801323225

[7] A.S. Garret, M.G. Corcos, *Leprosy Rev.* 23 (1952) 106-108. https://doi.org/10.5935/0305-7518.19520013

[8] J.G. Kublin, F.K. Dzinjalamala, D.D. Kamwendo, E.M. Malkin, J.F. Cortese, L.M. Martino, R.A.G. Mukadam, S.J. Rogerson, A.G. Lescano, M.E. Molyneux, P.A. Winstanley, P. Chimpeni, T.E. Taylor, C.V. Plowe, *J. Infect. Dis.* 185 (2002) 380-386. https://doi.org/10.1086/338566

[9] Y.I. Zhu, M.J. Stiller, *J. Am. Acad. Dermatol.* 45 (2001) 420-434. https://doi.org/10.1067/mjd.2001.114733

[10] D. Greenwood, in: R. Finch, D. Greenwood, R. Whitley, S. R. Norrby (Eds), *Antibiotic and Chemotherapy*, Elsevier, Netherlands 2011, pp. 337-343.

[11] M.V. Kachaeva, D.M. Hodyna, I.V. Semenyuta, S.G. Pilyo, V.M. Prokopenko, V.V. Kovalishym, L.O. Metelytsia, V.S. Brovarets, *Comput. Biol. Chem.* 74 (2018) 294-303. https://doi.org/10.1016/j.compbiolchem.2018.04.006

[12] L. Xu, J. Cheng, M.L. Trudell, *J. Org. Chem.* 68, (2003) *68*, 5388-5391. https://doi.org/10.1021/jo030031n

[13] P. Kowalski, K. Mitka, K. Ossowska, Z. Kolarska, *Tetrahedron* 61 (2005) 1933-1953. https://doi.org/10.1016/j.tet.2004.11.041

[14] F. Ruff, A. Fábián, Ö. Farkas, Á. Kucsman, *Eur. J. Org. Chem. 13 (*2009) 2102-2111. https://doi.org/10.1002/ejoc.200801180

[15] N.J. Leonard, C.R. Johnson, *J. Org. Chem.* 27 (1962) 282-284. https://doi.org/10.1021/jo01048a504

[16] R.D. Bach, M.D. Su, H.B. Schlegel, *J. Am. Chem. Soc. 116 (*1994) *116*, 5379-5391. https://doi.org/10.1021/ja00091a049

[17] S.J.H.F. Arts, E.J.M. Mombarg, H. van Bekkum, R.A. Sheldon, *Synthesis* 6 (1997) 597-613. https://doi.org/10.1055/s-1997-1406

[18] S.K.M. Islam, S. Paul, A.S. Roy, P. Mondal, *J. Inorg. Organomet. Polym. Mat.* 23 (2013) 560-570. https://doi.org/10.1007/s10904-012-9813-6

[19] H.Q.N. Gunaratne, M.A. McKervey, S. Feutren, J. Finlay, J. Boyd, *Tetrahedron Lett.* 39 (1998) 5655-5658. https://doi.org/10.1016/S0040-4039(98)01100-9

[20] Y. Mekmouche, H. Hummel, R.Y.N. Ho, L. Que Jr., V. Schünemann, F. Thomas, A.X. Trautwein, C. Lebrun, K. Gorgy, J.C. Lepretre, M.N. Collomb, A. Deronzier, M. Fontecave, S. Ménage, *Chem. Eur. J.* 8 (2002) 1196-1204. https://doi.org/10.1002/1521-3765(20020301)8:5<1196::AID-CHEM1196>3.0.CO;2-Z

[21] C.L. Hill, in: G. Strukul (Ed.), *Catalytic Oxidation with Hydrogen Peroxide as Oxidant* Springer, New York, 1992, pp. 253-280.

[22] R.A. Frenzel, Á.G. Sathicq, M.N. Blanco, G.P. Romanelli, L.R. Pizzio, *J. Mol. Catal. A: Chem.403 (*2015) 27-36. http://doi.org/10.1016/j.molcata.2015.02.021

[23] E. Kraleva, A. Spojakina, R. Edreva-Kardjieva, K. Jiratova, L. Petrov, *React. Kinet. Catal. Lett.* 92 (2007) 111-119. http://doi.org/10.1007/s11144-007-4896-8

[24] T. Ressler, U. Dorn, A. Walter, S. Schwarz, A. H. P. Hahn, *J. Catal. 275 (*2010) 1-10. http://doi.org/10.1016/j.jcat.2010.07.001

[25] M.S. Kuyukina, I.B. Ivshina, A.Y. Gavrin, E.A. Podorozhko, V.I. Lozinsky, C.E. Jeffree, J.C. Philp, *J. Microbiol. Methods* 65 (2006) 596-603. http://doi.org/10.1016/j.mimet.2005.10.006

[26] V.I. Lozinsky, A.L. Zubov, E.F. Titova, *Enzyme Microb. Technol.* 20 (1997) 182-190. https://doi.org/10.1016/S0141-0229(96)00110-X

[27] A. Aires-Trapote, P. Hoyos, A.R. Alcantara, A. Tamayo, J. Rubio, A. Rumbero, M.J. Herna, *Org. Process Res. Dev. 19 (*2015) 687-694. https://doi.org/10.1021/op500326k

[28] N. Sahiner, F. Seven, *Energy 71* (2014) 170-179. https://doi.org/10.1016/j.energy.2014.04.031

[29] M.U. Ashraf, M.A. Hussain, G. Muhammad, M.T. Haseeb, S. Bashir, S.Z. Hussain, I. Hussain, *Int. J. Biol. Macromol.* 95 (2017) 138-144. http://doi.org/10.1016/j.ijbiomac.2016.11.057

[30] U. Bertram, R. Bodmeier, *Eur. J. Pharm. Sci.* 27 (2006) 62-71. https://doi.org/10.1016/j.ejps.2005.08.005

[31] H. Omidian, K. Park, J.G. Roca, *J. Pharm. Pharmacol. 59 (*2007) 317-327. https://doi.org/10.1211/jpp.59.3.0001

[32] V. Palermo, Á.G. Sathicq, T. Constantieux, J. Rodríguez, P.G. Vázquez, G.P. Romanelli, *Catal. Lett. 146 (*2016) 1634-1647. https://doi.org/10.1007/s10562-016-1784-8

[33] P.J. Domaille, *J. Amer. Chem. Soc.* 106 (1994) 7677-7687. https://doi.org/10.1021/ja00337a004

[34] J. Canny, R. Thouvernot, A. Tézé, G. Hervé, M. Leparuolo-Loftus, *Inorg. Chem.* 30 (1991) 976-981. https://doi.org/10.1021/ic00005a020

[35] B. Ma, Z. Zhang, W. Song, X. Xue, Y. Yu, Z. Zhao, Y. Ding, *J. Mol. Catal. A: Chem. 368-369 (*2013) 152-158. https://doi.org/10.1016/j.molcata.2012.11.022

[36] R. Frenzel, D. Morales, G. Romanelli, G. Sathicq, M. Blanco, L. Pizzio, *J. Mol. Catal. A: Chem.* 420 (2016) 124-133. https://doi.org/10.1016/j.molcata.2016.01.026

[37] P. Kubelka, F. Munk, *Z. Tech. Phys.* 12 (1931) 593-601. (English translation by S. Westin http://www.graphics.cornell.edu/~westin/pubs/kubelka.pdf)

[38] D.R. Park, S. Park, Y. Bang, I.K. Song, *Appl. Catal. A: Gen.* 373 (2010) 201-207. https://10.1016/j.apcata.2009.11.018

[39] R. Cid, G. Pecchi, *Appl. Catal.* 14 (1985) 15-21. https://doi.org/10.1016/S0166-9834(00)84340-7

[40] L. Méndez, R. Torviso, L. Pizzio, M. Blanco, *Catal. Today 173 (*2011) 32-37. https://10.1016/j.cattod.2011.03.028

[41] L.R. Pizzio, M.N. Blanco, *Micropor. Mesopor. Mat.* 103 (2007) 40-47. https://10.1016/j.micromeso.2007.01.036

[42] T. Huang, N. Tian, Q. Wu, W. Yan, *Soft. Matter.* 11 (2015) 4481-4486. https://10.1039/C5SM00298B

[43] R. de Paiva Floro Bonfim, L.C. de Moura, H. Pizzala, S. Caldarelli, S. Paul, J.G. Eon, O. Mentré, M. Capron, L. Delevoye, E. Payen, *Inorg. Chem. 46 (*2007) 7371-77. https://doi.org/10.1021/ic700384m

[44] R. Thouvernot, M. Fournier, R. Franck, C. Rocchiccioli-Deltcheff, *Inorg. Chem.* 23 (1984) 598-605. https://doi.org/10.1021/ic00173a022

[45] W. Trakarnpruk, J. Jatupisarnpong, *Appl. Petrochem. Res.* 3 (2013) 9-15. https://doi.org/10.1007/s13203-012-0023-5

[46] E.O.J. Gultom, A. Lesbani, *Sci. Technol. Indonesia 2* (2017) 50-55. https://doi.org/10.26554/sti.2017.2.2.50-55

[47] W. Huang, L. Todaro, G.P.A. Yap, R. Beer, L.C. Francesconi, T. Polenova, *J. Am. Chem. Soc.* 126 (2004) 11564-11573. https://doi.org/10.1021/ja0475499

[48] P. Mothé-Esteves, M. Maciel Pereira, J. Arichi, B. Louis, *Cryst. Growth Des.* 10 (2010) 371-378. https://doi.org/10.1021/cg900984z

[49] D.R. Park, S.H. Song, U.G. Hong, J.G. Seo, J.G. Jung, I.K. Song, *Catal. Lett.* 132 (2009) 363-369. https://doi.org/10.1007/s10562-009-0114-9

[50] R.A. Frenzel, G.P. Romanelli, L.R. Pizzio, *J. Mol. Catal. 457 (*2018) 8-16. https://doi.org/10.1016/j.mcat.2018.07.016

[51] V. Palermo, Á. Sathicq, T. Constantieux, J. Rodríguez, P. Vázquez, G. Romanelli, *Catal. Lett.* 145 (2015) 1022-1032. https://doi.org/10.1007/s10562-015-1498-3

[52] O. D'alessandro, G. Sathicq, V. Palermo, L. M. Sanchez, H. Thomas, P. Vazquez, T. Constantieux, G. Romanelli, *Curr. Org. Chem.* 16 (2012) 2763-2736. https://doi.org/10.2174/138527212804546840

[53] G.W. Raiziss, L.W. Clemence, M. Severac, J.C. Moetsch, *J. Am. Chem. Soc.* 61 (1939) 2763-2765. https://doi.org/10.1021/ja01265a060

[54] A.M. Van Arendonk, E.C. Kleiderer, *J. Am. Chem. Soc. 62 (*1940) 3521-3522. https://doi.org/10.1021/ja01869a509

[55] M. Villa, C. De Faveri, R. Zanotti, F. Ciardella, F. Borin, (Lundbeck Pharmaceuticals Italy S.P.A.) (2006) WO 2006002690 A1

TABLES

Table 1. S_{BET}, Dp, and PSD of SPH, SiPV1, SiPV2, and SPH-SPOV using nitrogen adsorption-desorption isotherm

Compound	S_{BET} (m^2/g)	Dp (nm)	PSD (nm)*	
			Small mesopores	Large mesopores
SiPV1	5	-	-	
SiPV2	10	-	-	
SPH	341	13.5	3.6	16.2
SPH-SiPV1-10	330	13.5	3.7	15.9
SPH-SiPV2-10	335	13.2	3.6	16.0
SPH-SiPV1-20	318	12.9	3.4	16.5
SPH-SiPV2-20	310	12.8	3.5	16.1
SPH-SiPV1-30	305	12.9	3.4	16.0
SPH-SiPV2-30	300	12.8	3.5	16.2

*Maximum of the PSD

Table 2. Eg values of SiPV1, SiPV2, and the SPH-SPOV hybrid materials

Compound	**E_g (eV)**
SiP	3.02
SiPV1	2.17
SiPV2	2.07
SPH-SiPV1-10	2.90
SPH-SiPV2-10	2.88
SPH-SiPV1-20	2.84
SPH-SiPV2-20	2.72
SPH-SiPV1-30	2.78
SPH-SiPV2-30	2.60

Table 3. Homogeneous catalytic reaction using SiPV1 and SiPV2 in the oxidation of DPS[a]

Entry	Catalyst	Sulfide Conversion (%)[b]	Sulfoxide Selecivity (%)[b,c]	Sulfone Selectivity (%)[b,d]
1[e]	None	5	100	-
2[f]	SPH	7	100	-
3	SiPV1	66	58	42
4	SiPV2	96	60	40

[a] 1 mmol DPS, 5 mL acetonitrle, 1 mL of H_2O_2 35%w/v, 1% mmol of catalyst, 25°C, 7 h

[b] Measured by gas chromatography on the crude reaction mixture.

[c] Sulfoxide Selectivity = sulfoxide/(sulfoxide + sulfone).

[d] Sulfone Selectivity = sulfone/(sulfoxide + sulfone).

[e] Blank test, 24 h

[f] 1 mmol DPS, 5 mL acetonitrile, 1 mL of H_2O_2 35% w/v, 1% mmol of SPH, 25°C, 24 h

Table 4. Oxidation reaction of DPS using SiPV1 and SiPV2 as homogeneous catalysts at different reaction times[a]

Entry	Catalyst	Time (h)	Sulfide Conversion (%)[b]	Sulfoxide Selectivity (%)[b,c]	Sulfone Selectivity (%)[b,d]
1	SiPV1	5	52	76	24
		7	66	58	42
		9	70	52	48
		24	100	-	100
2	SiPV2	5	89	78	22
		7	96	60	40
		9	100	-	100
		24	100	-	100

[a] 1 mmol DPS, 1% mmol of SPOV, 5 mL acetonitrile, 1 mL of H_2O_2 35% w/v, 25°C

[b] Measured by gas chromatography on the crude reaction mixture.

[c] Sulfoxide Selectivity = sulfoxide/(sulfoxide + sulfone).

[d] Sulfone Selectivity = sulfone/(sulfoxide + sulfone).

Table 5. Oxidation reaction of DPS using variable amount of SiPV2 as catalyst[a]

Entry	Catalyst amount %	Sulfide Conversion (%)[b]	Sulfoxide Selectivity (%)[b,c]	Sulfone Selectivity (%)[b,d]
1	0.5	45	85	15
2	0.7	70	81	19
3	1	96	60	40
4	1.5	98	58	42

[a]1 mmol of DPS, 5 mL of acetonitrile, 1 mL H_2O_2 35% w/v, 25°C temperature and variable amount of SiPV2 as catalysts (0.5%, 0.7%, 1%, and 1.5% mmol), 7 h

[b] Measured by gas chromatography on the crude reaction mixture.

[c] Sulfoxide Selectivity = sulfoxide/(sulfoxide + sulfone).

[d] Sulfone Selectivity = sulfone/(sulfoxide + sulfone).

Table 6. Oxidation of DPS using SiPV2 as catalysts and different ratios substrate/H_2O_2 35% w/v[a]

Entry	Substrate/H_2O_2	Sulfide Conversion (%)[b]	Sulfoxide Selectivity (%)[b,c]	Sulfone Selectivity (%)[b,d]
1	1:3	70	68	32
2	1:5	75	58	42
3	1:7	85	20	80
4	1:10	100	-	100

[a] 1 mmol DPS, 5 mL acetonitrile, 1% mmol of SiPV2, 25°C and variable ratio substrate/H_2O_2 (1:3, 1:5, 1:7, and 1:10), 9 h

[b] Measured by gas chromatography on the crude reaction mixture.

[c] Sulfoxide Selectivity = sulfoxide/(sulfoxide + sulfone).

[d] Sulfone Selectivity = sulfone/(sulfoxide + sulfone).

Table 7. Oxidation of DPS using the synthesized materials SPH-SiPV1-X and SPH-SiPV2-X[a]

Entry[a]	Catalyst	Sulfide conversion (%)[b]	Sulfoxide Selectivity (%)[b,c]	Sulfone Selectivity (%)[b,c]
1	SPH	7	100	-
2	SPH-SiPV1-10	38	14	86
3	SPH-SiPV1-20	57	10	90
4	SPH-SiPV1-30	79	-	100
5	SPH-SiPV2-10	52	13	87
6	SPH-SiPV2-20	61	5	95
7	SPH-SiPV2-30	94	-	100

[a]1 mmol DPS, 5 mL acetonitrile, 1% mmol of SPH/SPH-SPOV-X, 25°C, 1 mL H_2O_2 35% w/v, 24 h

[b] Measured by gas chromatography on the crude reaction mixture.

[c] Sulfoxide Selectivity = sulfoxide/(sulfoxide + sulfone).

[d] Sulfone Selectivity = sulfone/(sulfoxide + sulfone).

Table 8. Reuse of catalysts SPH-SiPV1-30 and SPH-SiPV2-30[a]

Entry	Catalyst	N° of cycle	Sulfide Conversion (%)[b]	Sulfoxide Selectivity (%)[b,c]	Sulfone Selectivity (%)[b,d]
1	SPH-SiPV1-30	1	79	-	100
		2	78	2	98
		3	77	-	100
2	SPH-SiPV2-30	1	94	-	100
		2	94	-	100
		3	91	-	100

[a] 1 mmol DPS, 5 mL acetonitrile, 1% mmol of SPH-SiPV1-30 or SPH-SiPV2-30, 1 mL H_2O_2, 25°C, 24 h

[b] Measured by gas chromatography on the crude reaction mixture.

[c] Sulfoxide Selectivity = sulfoxide/(sulfoxide + sulfone).

[d] Sulfone Selectivity = sulfone/(sulfoxide + sulfone).

Table 9. SiPV2 leaching evaluation from SPH-SiPV2-30

Entry	Test	Sulfide Conversion (%)[a]	Sulfoxide Selectivity (%)[a,b]	Sulfone Selectivity (%)[a,c]
1[d]	SPH-SiPV2-30	94	-	100
2[e]	Refluxed SPH-SiPV2-30	92	-	100
3[f]	Refluxed acetonitrile	10	100	-

[a] Measured by gas chromatography on the crude reaction mixture.

[b] Sulfoxide Selectivity = sulfoxide/(sulfoxide + sulfone).

[c] Sulfone Selectivity = sulfone/(sulfoxide + sulfone).

[d] Reaction conditions: 1 mmol DPS, 5 mL acetonitrile, 1% mmol of SPH-SiPV2-30, 1 mL H_2O_2, 25°C, 24 h

[e] SPH-SiPV2-30 was stirred in 5mL of acetonitrile for 24 h, filtered, dried under reduced pressure until constant weight and use in a fresh reaction with the same conditions as [d].

[f] The acetonitrile obtained in point [e] was used as solvent in a fresh reaction with the same reaction conditions in [d], without the use of catalyst.

Table 10. Different methods used for dapsone synthesis

Entry	Reaction conditions	Number of steps	Yield (%)	Bibliography
1	H_2O_2 35% w/v SPH-SiPV2-30 25ºC	1	72	Present work
2	1) Glacial ACOH/Ac. anhydride 2) KCr_2O_7/H_2SO_4 3) HCl reflux	3	55-60	Raiziss et al [53]
3	1) Glacial AcOH/Ac. anhydride 2) Superoxol, boiling temp 3) HCl, reflux	3	70 (Crude)	Van Arendonk et al [54]
4	1) Glacial AcOH/acetic anhydride 2) H_2O_2/Na_2WO_4, 85ºC 3) H_2, Pd/C, HCl	3	82	Villa et al [55]

SCHEME & FIGURE CAPTIONS

Scheme 1. Oxidation reaction of diphenyl sulfide (DPS)

Scheme 2. Dapsone structure

Scheme 3. Oxidation reaction of 4,4'-diaminodiphenyl sulfide to dapsone

Figure 1. FTIR spectra of SiP, SiPV1, and SiPV2

Figure 2. FTIR spectra of SPH, SPH-SiPV1-10, SPH-SiPV1-20, SPH-SiPV1-30, and SiPV1 (normalized to the 1630 cm^{-1} band)

Figure 3. FTIR spectra of SPH, SPH-SiPV2-10, SPH-SiPV2-20, SPH-SiPV2-30, and SiPV2 (normalized to the 1630 cm^{-1} band)

Figure 4. Raman spectra of SiPV1 (A) and SiPV2 (B)

Figure 5. ^{51}V MAS-NMR spectra of SiPV1 (A) and SiPV2 (B)

Figure 6. SEM micrographs of SPH (A) and SPH-SiPV1-30 (B) samples.

Figure 7. DRS-UV-vis spectra of SiP, SiPV1, SiPV2, SPH, SPH-SiPV1-10, SPH-SiPV1-20, SPH-SiPV1-30, SPH-SiPV2-10, SPH-SiPV2-20, and SPH-SiPV2-30

Figure 8. Potentiometric titration with *n*-butylamine of SPH, SiPV1, and SPH-SiPV1-X (A) SPH, SiPV2, and SPH-SiPV2-X (B)

Figure 9. DPS Conversion vs. amount of SiPV2

SCHEMES & FIGURES

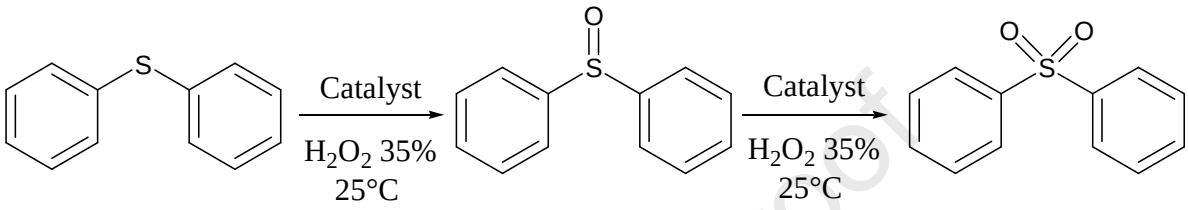

Scheme 1. Oxidation reaction of diphenyl sulfide (DPS)

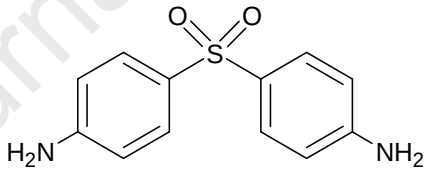

Scheme 2. Dapsone structure

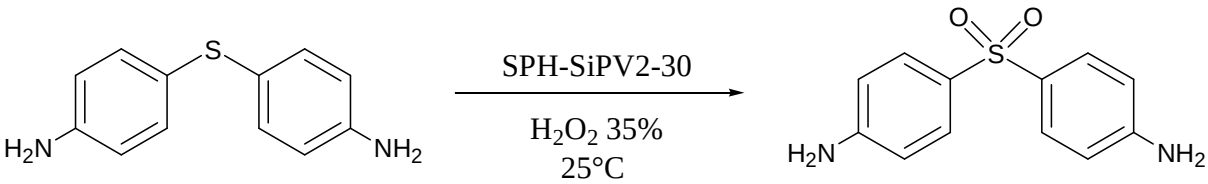

Scheme 3. Oxidation reaction of 4,4'-diaminodiphenyl sulfide to dapsone

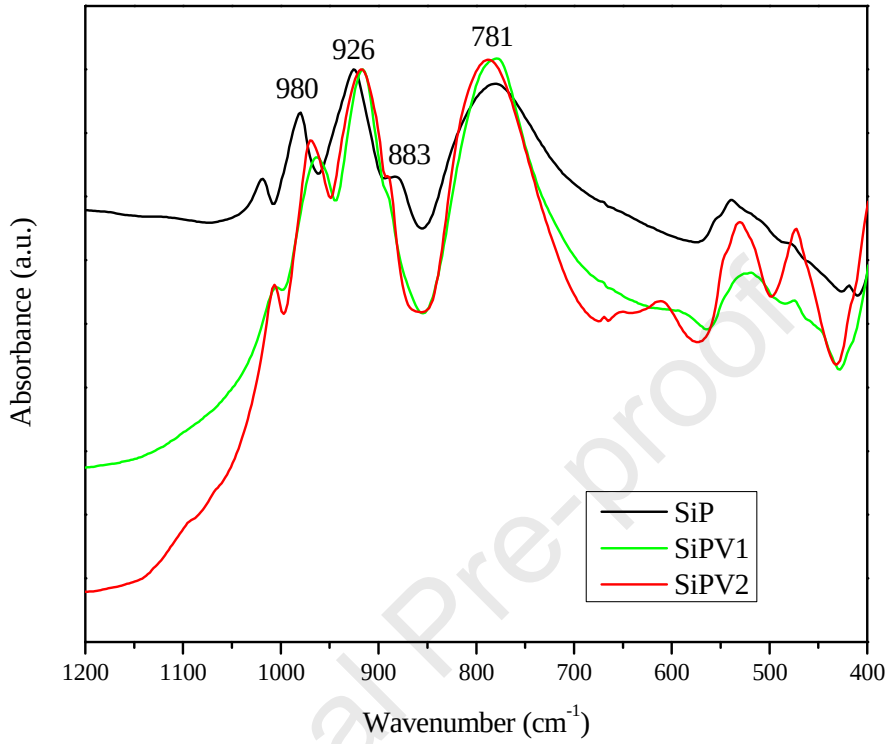

Figure 1. FTIR spectra of SiP (black line), SiPV1 (green line), and SiPV2 (red line).

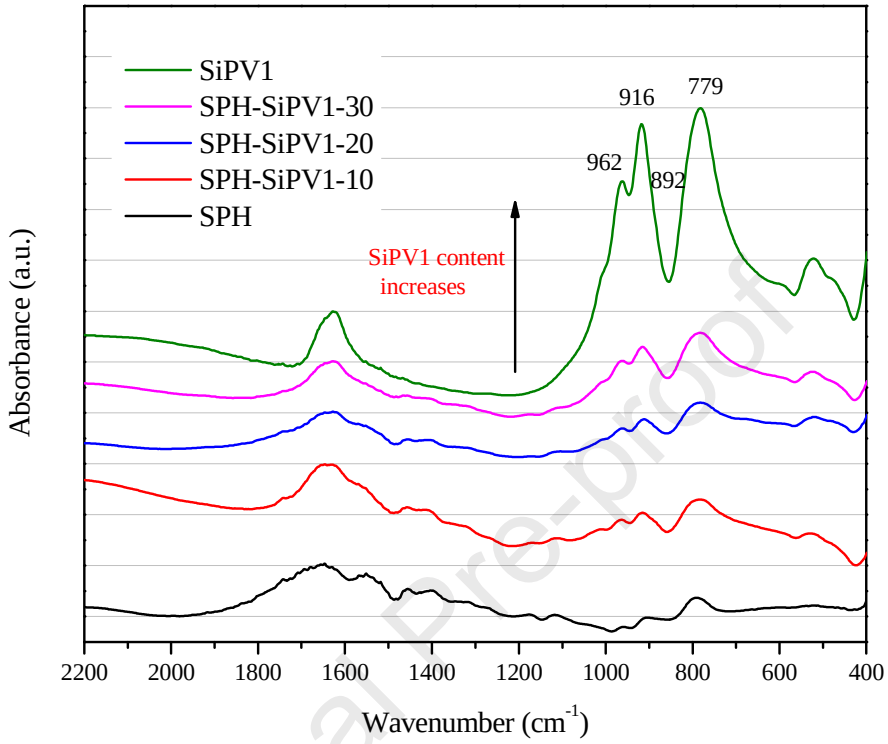

Figure 2. FTIR spectra of SPH (black line, bottom), SPH-SiPV1-10 (red line, second from bottom), SPH-SiPV1-20 (blue line, third from bottom), SPH-SiPV1-30 (pink line fourth from bottom), and SiPV1 (green line, top), all normalized to the 1630 cm^{-1} band.

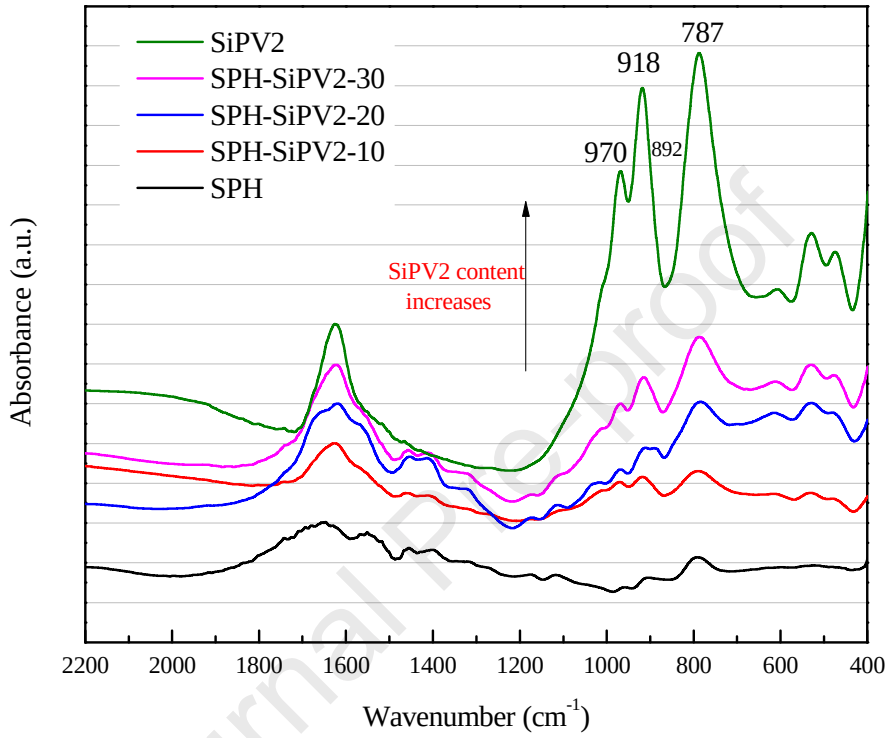

Figure 3. FTIR spectra of SPH (black line, bottom), SPH-SiPV2-10 (red line, second from bottom), SPH-SiPV2-20 (blue line, third from bottom), SPH-SiPV2-30 (pink line fourth from bottom), and SiPV2 (green line, top), all normalized to the 1630 cm^{-1} band.

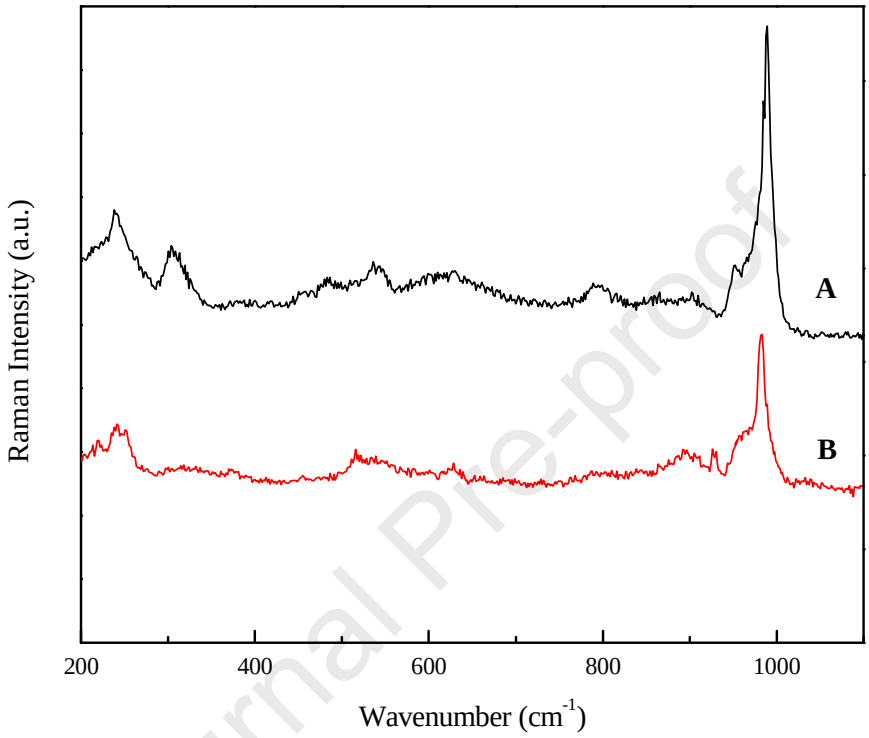

Figure 4. Raman spectra of SiPV1 (A) and SiPV2 (B)

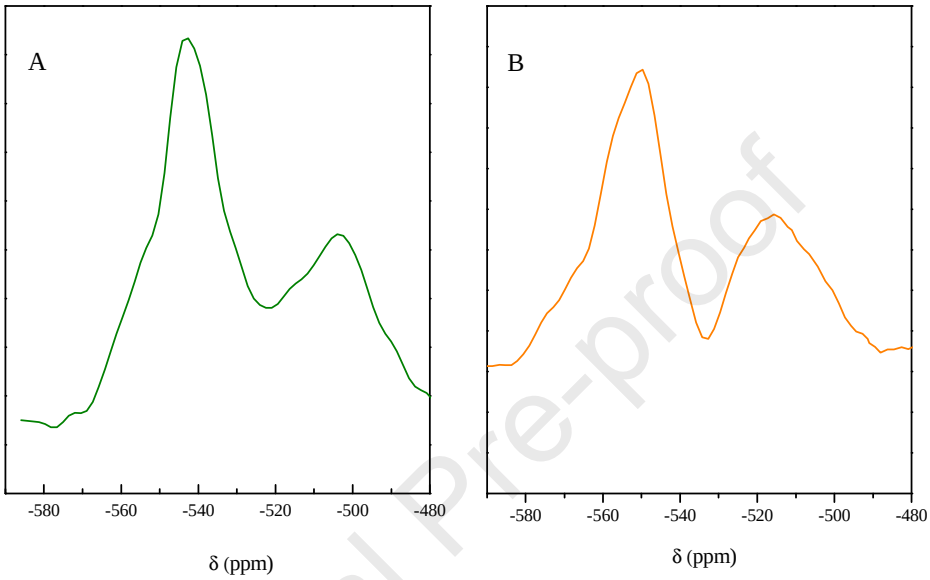

Figure 5. ^{51}V MAS-NMR spectra of SiPV1 (A) and SiPV2 (B)

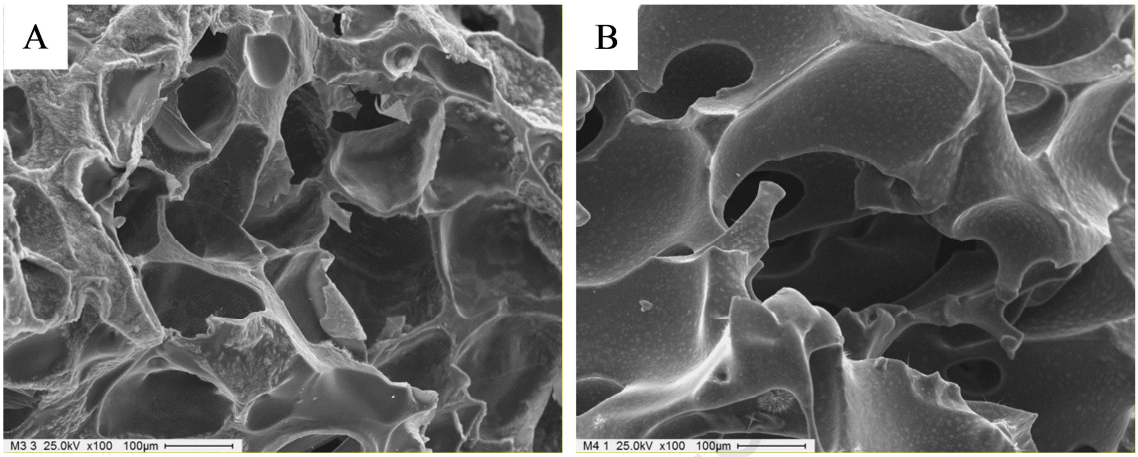

Figure 6. SEM micrographs of SPH (A) and SPH-SiPV1-30 (B) samples.

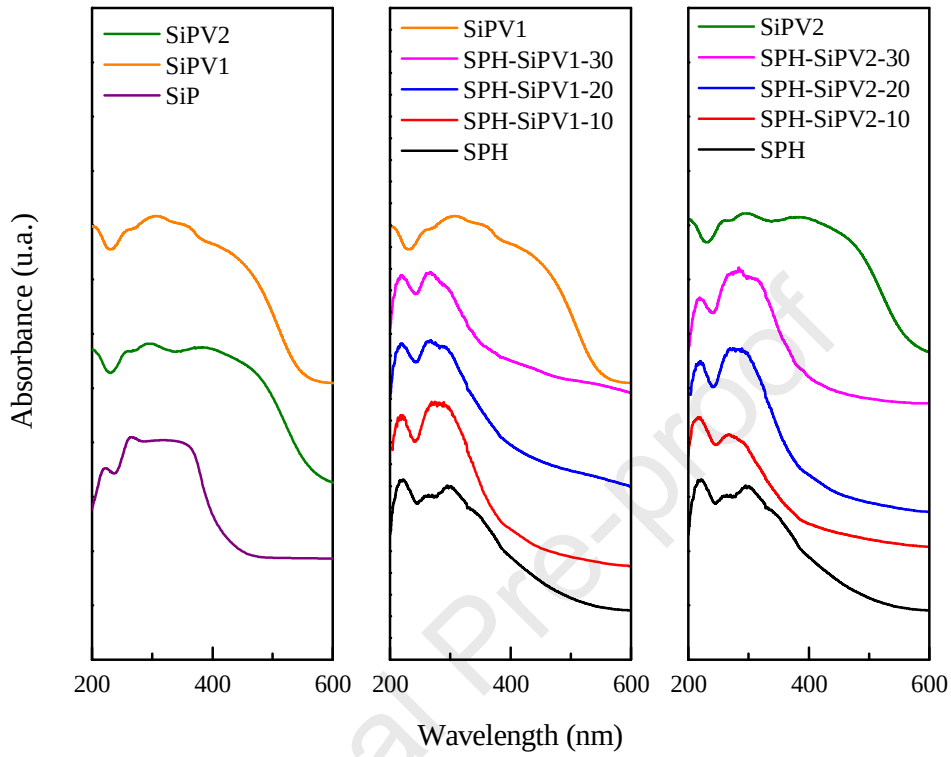

Figure 7. DRS-UV-vis spectra of SiP, SiPV1, SiPV2, SPH, SPH-SiPV1-10, SPH-SiPV1-20, SPH-SiPV1-30, SPH-SiPV2-10, SPH-SiPV2-20, and SPH-SiPV2-30

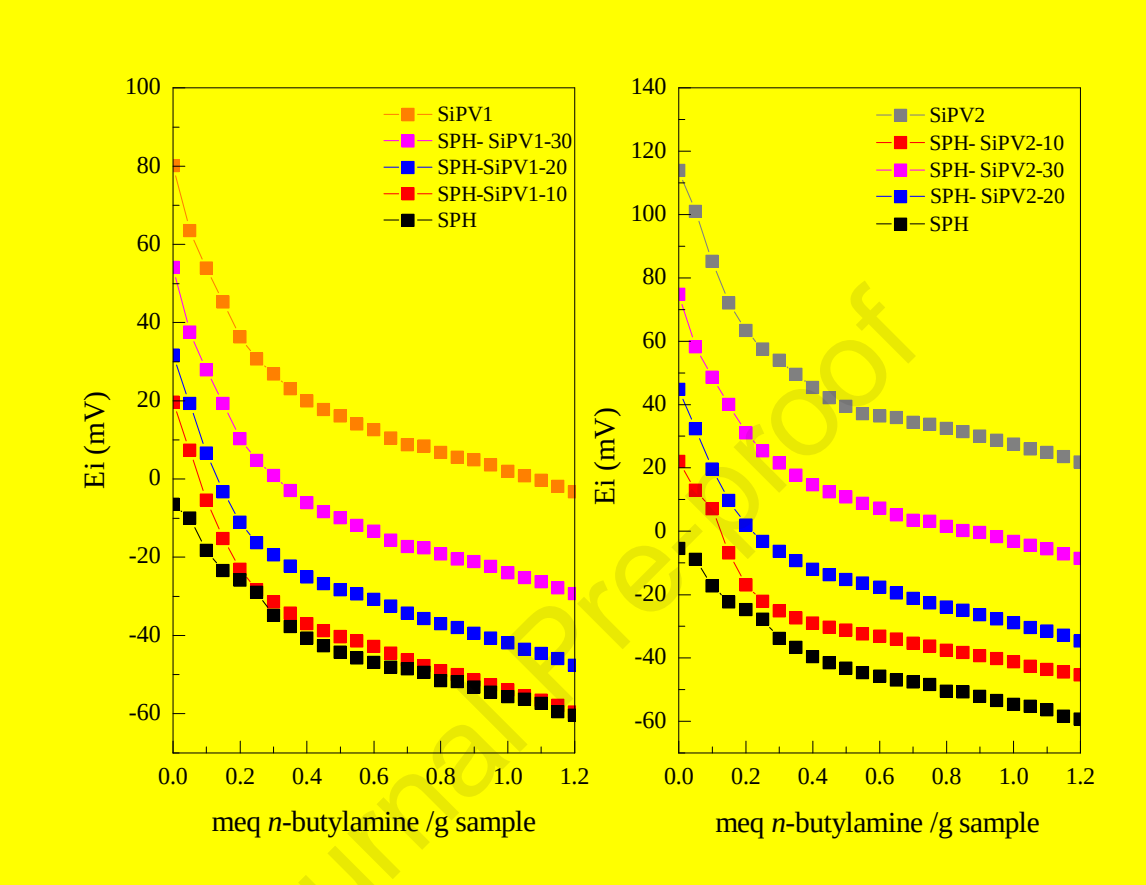

Figure 8. Potentiometric titration with *n*-butylamine of SPH, SiPV1, and SPH-SiPV1-X (A) SPH, SiPV2, and SPH-SiPV2-X (B)

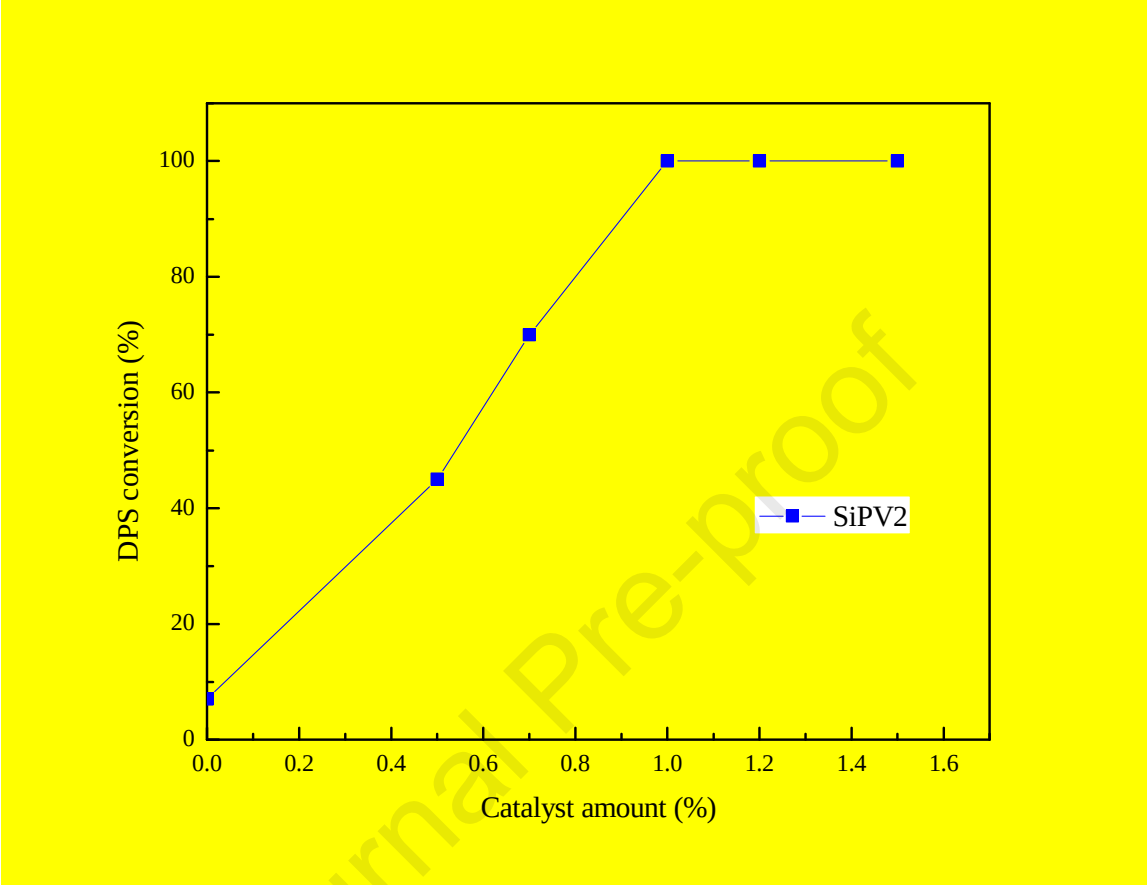

Figure 9. DPS Conversion vs. amount of SiPV2

GRAPHICAL ABSTRACT. Polyoxometalate incorporated in a superporous hydrogel as heterogeneous catalyst in the selective oxidation of sulfides

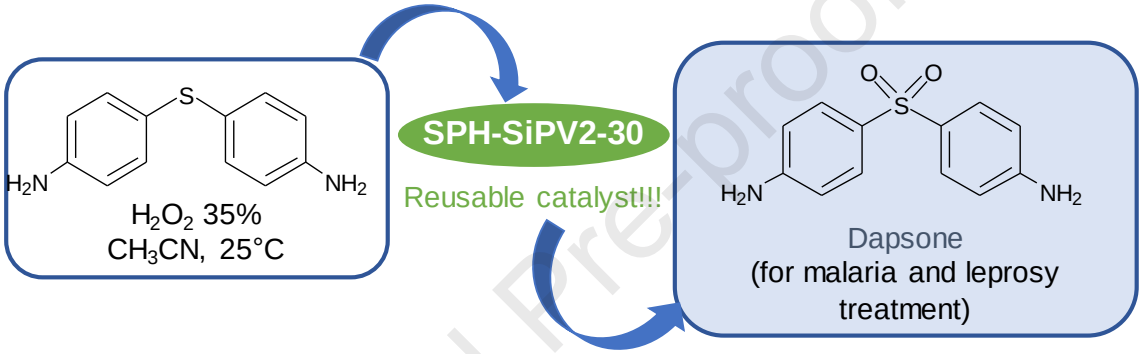

RESEARCH HIGHLIGHTS

Silicopolyoxotungstovanadates immobilized in a superporous hydrogel as catalyst.

Selective oxidation of sulfides by hydrogen peroxide using heterogeneous catalysis.

Green synthesis of dapsone, an important drug for malaria and leprosy treatment.

Declaration of interests

☒ The authors declare that they have no known competing financial interests or personal relationships that could have appeared to influence the work reported in this paper.

☐The authors declare the following financial interests/personal relationships which may be considered as potential competing interests: